Surface Layer of *Lactobacillus helveticus* MIMLh5 Promotes Endocytosis by Dendritic Cells

Valentina Taverniti,[a] Mauro Marengo,[a] Eva Fuglsang,[b] Helene Marie Skovsted,[b] (ID) Stefania Arioli,[a] Giacomo Mantegazza,[a] Giorgio Gargari,[a] Stefania Iametti,[a] Francesco Bonomi,[a] (ID) Simone Guglielmetti,[a] Hanne Frøkiær[b]

[a]Department of Food, Environmental, and Nutritional Sciences, Università degli Studi di Milano, Milan, Italy
[b]Department of Veterinary and Animal Sciences, University of Copenhagen, Copenhagen, Denmark

ABSTRACT Surface layers (S-layers) are proteinaceous arrays covering the cell walls of numerous bacteria. Their suggested properties, such as interactions with the host immune system, have been only poorly described. Here, we aimed to elucidate the role of the S-layer from the probiotic bacterial strain *Lactobacillus helveticus* MIMLh5 in the stimulation of murine bone-marrow-derived dendritic cells (DCs). MIMLh5 induced greater production of interferon beta (IFN-β), interleukin 10 (IL-10), and IL-12p70, compared to S-layer-depleted MIMLh5 (naked MIMLh5 [n-MIMLh5]), whereas the isolated S-layer was a poor immunostimulator. No differences in the production of tumor necrosis factor alpha (TNF-α) or IL-1β were found. Inhibition of the mitogen-activated protein kinases JNK1/2, p38, and ERK1/2 modified IL-12p70 production similarly in MIMLh5 and n-MIMLh5, suggesting the induction of the same signaling pathways by the two bacterial preparations. Treatment of DCs with cytochalasin D to inhibit endocytosis before the addition of fluorescently labeled MIMLh5 cells led to a dramatic reduction in the proportion of fluorescence-positive DCs and decreased IL-12 production. Endocytosis and IL-12 production were only marginally affected by cytochalasin D pretreatment when fluorescently labeled n-MIMLh5 was used. Treatment of DCs with fluorescently labeled S-layer-coated polystyrene beads (Sl-beads) resulted in much greater uptake of beads, compared to noncoated beads. Prestimulation of DCs with cytochalasin D reduced the uptake of Sl-beads more than plain beads. These findings indicate that the S-layer plays a role in the endocytosis of MIMLh5 by DCs. In conclusion, this study provides evidence that the S-layer of *L. helveticus* MIMLh5 is involved in endocytosis of the bacterium, which is important for strong Th1-inducing cytokine production.

IMPORTANCE Beneficial microbes may positively affect host physiology at various levels, e.g., by participating in immune system maturation and modulation, boosting defenses and dampening reactions, thus affecting the whole homeostasis. As a consequence, the use of probiotics is increasingly regarded as suitable for more extended applications for health maintenance, not only microbiota balancing. This implies a deep knowledge of the mechanisms and molecules involved in host-microbe interactions, for the final purpose of fine tuning the choice of a probiotic strain for a specific outcome. With this aim, studies targeted to the description of strain-related immunomodulatory effects and the identification of bacterial molecules responsible for specific responses are indispensable. This study provides new insights in the characterization of the food-origin probiotic bacterium *L. helveticus* MIMLh5 and its S-layer protein as a driver for the cross-talk with DCs.

KEYWORDS MAPKs, cytochalasin D, cytokines, nanoparticles, probiotic

Surface layers (S-layers) are bidimensional crystalline arrays of proteins that form an outer self-assembled envelope on the bacterial cell wall. S-layer proteins are ubiquitously present in archaea and Gram-positive and Gram-negative bacteria (1). They are composed of numerous identical subunits forming a symmetrical, porous, lattice-like layer that completely covers the cell surface. Considering the metabolic efforts that S-layer biogenesis, translocation, and assembly imply for bacterial cells, these proteins are expected to have important functions for the organism. Several studies have demonstrated different functions connected to the presence of S-layer proteins on bacterial surfaces, such as virulence, adhesion, protection, degradative activities (e.g., amidase), and molecular sieving (2). Among beneficial bacteria, several *Lactobacillus* species are equipped with S-layer proteins, including *Lactobacillus helveticus*. In comparison with other bacteria, *Lactobacillus* S-layer proteins are characterized by their small size and high pI values (3). Mostly, S-layers of lactobacilli have been shown to have adhesive (4, 5) and immunomodulatory (6–9) properties. However, our understanding of the role of S-layers in immunomodulation is still limited.

We previously described *L. helveticus* MIMLh5 as a probiotic strain (10–13). We also reported that the isolated S-layer protein induced the expression of tumor necrosis factor alpha (TNF-α) and cyclooxygenase 2 (COX-2) in the human monocyte-derived cell line U937 and in murine bone marrow-derived and peritoneal cavity-isolated macrophages (7). In those studies, we observed that depletion of the S-layer from the surface of *L. helveticus* MIMLh5 decreased the ability of the bacterium to induce TNF-α and COX-2 expression but did not alter the expression of interleukin 10 (IL-10). In contrast, Konstantinov and collaborators demonstrated a role of the S-layer (SlpA) from *Lactobacillus. acidophilus* NCFM in eliciting the production of the anti-inflammatory cytokine IL-10 in human dendritic cells (DCs) via interaction with the C-type lectin DC-SIGN receptor, whereas a more proinflammatory profile emerged in the presence of an *L. acidophilus* NCFM knockout mutant lacking SlpA (9).

DCs use two different strategies that are dependent on actin polymerization to endocytose bacteria and other particles larger than 800 nm, i.e., (i) phagocytosis, an endocytic process that requires the interaction between multiple microbial ligands and DCs receptors (14), and (ii) macropinocytosis, a nonspecific uptake of components present in the surrounding fluid (15). Reportedly, endocytosis of *Lactobacillus acidophilus* NCFM by bone marrow-derived DCs induced interferon beta (IFN-β) production, which in turn activated the expression of numerous genes, including IL-12 (16, 17). In addition, evidence that both phagocytosis and constitutive macropinocytosis contributed to the uptake of strain NCFM was provided (18). Lack of stimulation of plasma membrane Toll-like receptors (TLRs) prior to endocytosis was also shown to be a prerequisite for strong IFN-β/IL-12p70 induction (18) by *L. acidophilus* NCFM, whose S-layer protein shares a high level of similarity with that of *L. helveticus* MIMLh5 (73% identity and 83% positivity) (19).

Here we investigated the role of the MIMLh5 S-layer in the induction of IL-12p70 production by DCs and its possible role in endocytosis of the bacterium, by comparing the effects of DC stimulation with untreated MIMLh5 and S-layer-depleted MIMLh5 (naked MIMLh5 [n-MIMLh5]). We also tested the purified MIMLh5 S-layer protein and S-layer-coated polystyrene beads (Sl-beads) (~800-nm diameter) to mimic the interaction of the protein with immune cells when the protein is anchored on the surface of particles with the size of a bacterium.

RESULTS

Depletion of the S-layer from *L. helveticus* MIMLh5 reduces IFN-β, IL-12p70, and IL-10 production by DCs. To study the role of the S-layer protein in the *L. helveticus* MIMLh5-mediated induction of a Th1-activating response in DCs, we compared the levels of different cytokines produced by DCs upon stimulation with *L. helveticus* MIMLh5 or n-MIMLh5. SDS-PAGE confirmed that the protein was efficiently removed from the bacterial surface, as evidenced by the strong reduction of the 45-kDa band corresponding to the MIMLh5 S-layer protein, while the other proteins were left
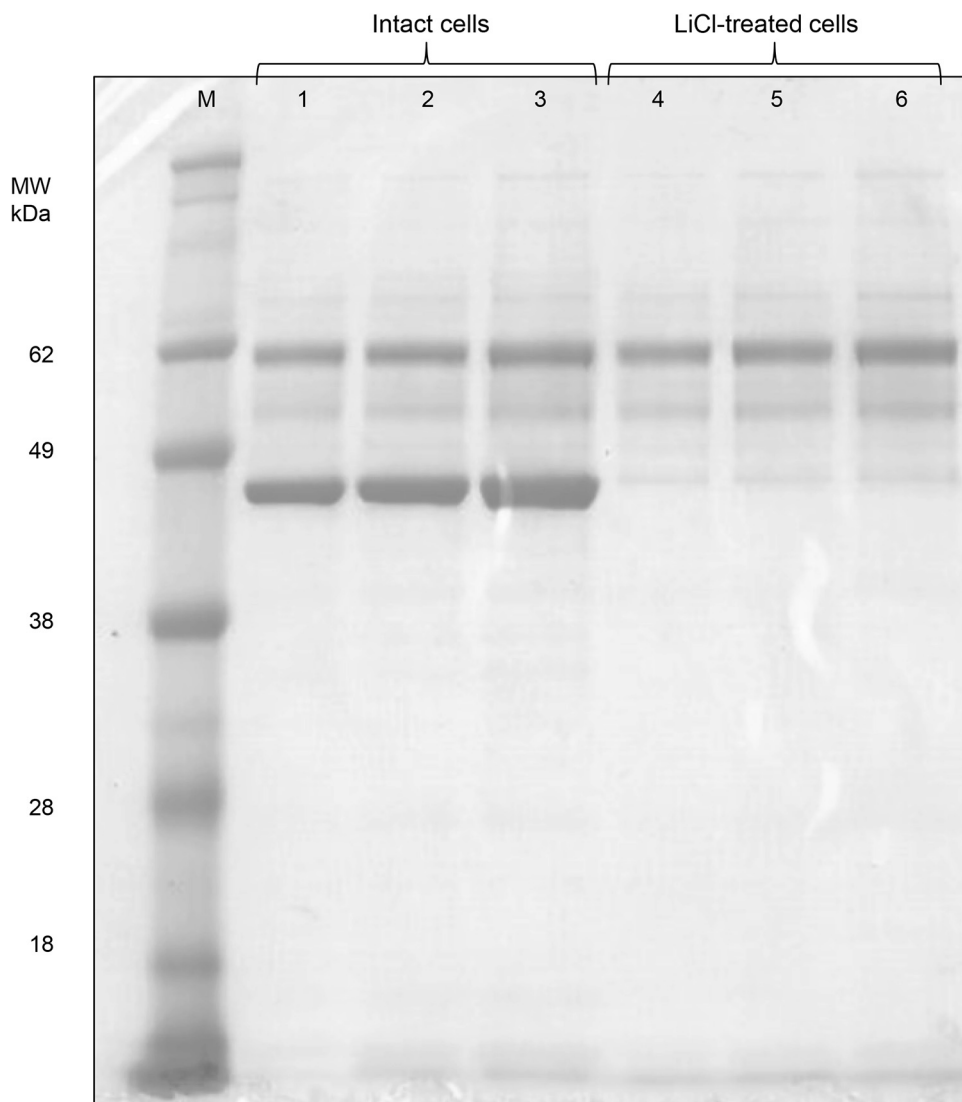
FIG 1 SDS-PAGE profiles of crude cell extracts obtained by boiling *L. helveticus* MIMLh5 cells before and after LiCl treatment. M, molecular weight markers. Lanes 1 to 3, extracts from 2.5×10^8, 3.75×10^8, and 5×10^8 intact MIMLh5 cells, respectively; lanes 4 to 6, extracts from 2.5×10^8, 3.75×10^8, and 5×10^8 LiCl-treated MIMLh5 cells, respectively.

apparently unaltered (Fig. 1, lanes 4 to 6). Then, the expression of the IFN-β, IL-12p35, IL-10, TNF-α, and IL-1β genes in DCs at 2, 4, 6, and 10 h was analyzed by reverse transcription (RT)-quantitative PCR (qPCR) following stimulation with bacteria and the S-layer protein; furthermore, the concentrations of the corresponding cytokines were assessed by enzyme-linked immunosorbent assays (ELISAs) in DC supernatants collected after 10 h of incubation.

Removal of the S-layer protein from the surface of MIMLh5 cells influenced the ability of the bacterium to induce IFN-β, IL-12p35, IL-10, TNF-α, and IL-1β gene expression (Fig. 2, top). ELISA data demonstrated that the levels of IFN-β, IL12p70, and IL-10 were significantly decreased in the supernatants of DCs stimulated with n-MIMLh5, compared to intact MIMLh5 (Fig. 2, bottom). The purified S-layer protein did not induce the expression of IFN-β or IL-12p35 genes at any of the time points considered (Fig. 2, top), as confirmed at the protein level by ELISA at 10 h (Fig. 2, bottom). In contrast, the S-layer protein induced the expression of the IL-10 gene and the proinflammatory cytokine TNF-α and IL-1β genes (Fig. 2, top), as confirmed by corresponding cytokine quantification in DC supernatants (Fig. 2, bottom). Overall,
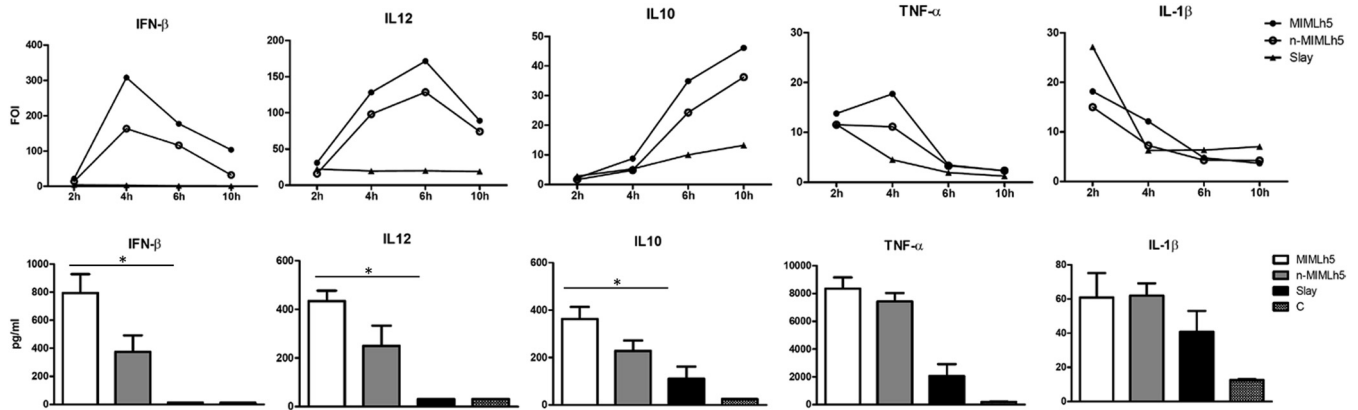
FIG 2 Cytokine profiles elicited in bone-marrow-derived DCs by *L. helveticus* MIMLh5 cells with and without (n-MIMLh5) S-layer and by purified S-layer protein. (Top) Expression of cytokine IFN-β, IL-12p35, IL-10, TNF-α, and IL-1β genes was determined by RT-qPCR after 2, 4, 6, and 10 h of incubation. Expression profiles are indicated as the fold change of induction (FOI) relative to the control (unstimulated DCs), which was set at a value of 1. (Bottom) IFN-β, IL-12p70, IL-10, TNF-α, and IL-1β protein levels were measured in the supernatants of DCs by ELISA after 10 h of incubation. Slay, S-layer protein from *L. helveticus* MIMLh5 was used at a concentration of 10 μg ml^{-1}. MIMLh5 and n-MIMLh5 cells were both used at a MOI of 50. C, control (unstimulated DCs). Data represent means ± standard deviations of triplicate measurements. Asterisks indicate statistically significant differences between MIMLh5 and n-MIMLh5, according to unpaired *t* tests. *, $P < 0.05$.

n-MIMLh5 induced the same cytokine expression profiles as MIMLh5 but to a lesser extent (Fig. 2, top). The cytokine concentrations in the supernatants harvested after 10 h reflected the expression profiles for each gene, with significant differences between n-MIMLh5 and MIMLh5 regarding IFN-β, IL-12p70, and IL-10 concentrations (Fig. 2, bottom).

The effects of MAPK inhibition on IL-12p70 production do not differ between MIMLh5 and n-MIMLh5. To test whether the *L. helveticus* MIMLh5 S-layer protein influences the signaling pathways that initiate IL-12 production by DCs, we investigated the effects of inhibiting specific mediators of the mitogen-activated protein kinase (MAPK) cascade (20), namely, JNK1/2, p38, and ERK1/2. These pathways were previously shown to be involved in *L. acidophilus* NCFM-dependent induction of IL-12 production in DCs (21, 22). The production of IL-12p70 was quantified by ELISA upon addition of MAPK inhibitors before bacterial stimulation. JNK1/2 inhibition resulted in 26% and 39% reductions of IL-12p70 levels upon stimulation with *L. helveticus* MIMLh5 and n-MIMLh5, respectively (Fig. 3). Inhibition of p38 lowered IL-12p70 production by 24% (MIMLh5) and 66% (n-MIMLh5), whereas blocking of ERK1/2 caused increases in IL-12p70 levels of 62% (MIMLh5) and 32% (n-MIMLh5) (Fig. 3).

Inhibition of bacterial endocytosis decreases IL-12p70 production in DCs stimulated with intact but not S-layer-depleted MIMLh5 cells. To test whether the
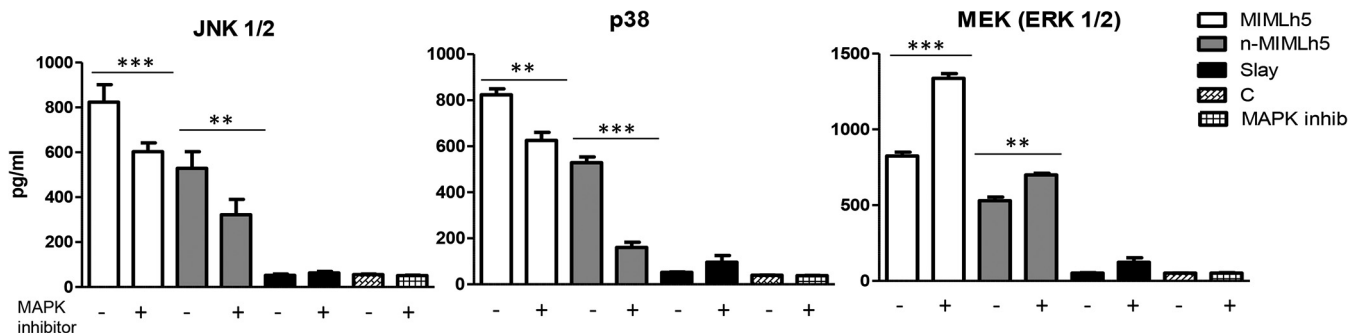

FIG 3 Stimulation of DCs with *L. helveticus* MIMLh5 cells, n-MIMLh5 cells, and the purified S-layer protein after preincubation with inhibitors for JNK1/2, p38, and MEK1/2. Cytokine IL-12p70 protein levels were measured in the supernatants of DCs by ELISA after 20 h. MIMLh5 and n-MIMLh5 were used at a MOI of 50. Slay, S-layer protein tested at a concentration of 10 μg ml^{-1}. C, control (unstimulated DCs). MAPK inhib, DCs stimulated only with the respective MAPK inhibitors for JNK, p38, and MEK. Asterisks indicate statistically significant differences, according to unpaired *t* tests. ***, $P < 0.001$; **, $P < 0.01$. Data represent means ± standard deviations of measurements from triplicate cultures.
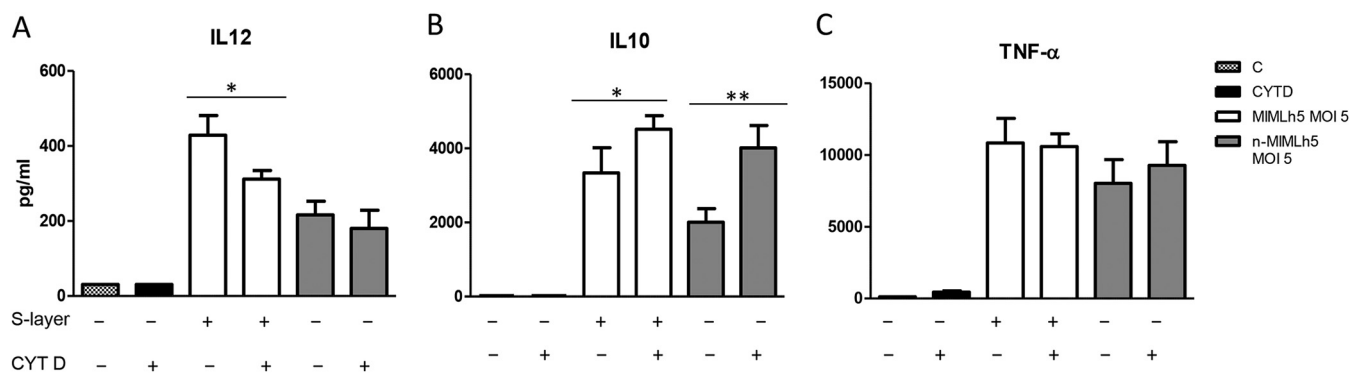
FIG 4 Cytokine production in DCs upon stimulation with *L. helveticus* MIMLh5 and n-MIMLh5 in the presence of cytochalasin D. DCs were prestimulated for 1 h with cytochalasin D (0.5 μg ml^{-1}) before the addition of bacterial cells. Protein levels of the cytokines IL-12p70 (A), IL-10 (B), and TNF-α (C) were measured in the supernatants of DCs by ELISA after 20 h. LiCl-treated and untreated MIMLh5 cells were used at a MOI of 5. n-MIMLh5, MIMLh5 cells after removal of the S-layer protein by LiCl extraction. C, control (unstimulated DCs). CYTD, DCs stimulated only with cytochalasin D. Asterisks indicate statistically significant differences, according to unpaired *t* tests. **, $P < 0.01$; *, $P < 0.05$. Data represent means $\pm$ standard deviations of measurements from triplicate cultures.

S-layer protein affects endocytosis of *L. helveticus* MIMLh5 by DCs, we quantified IL-12p70, IL-10, and TNF-α levels by ELISA after stimulation of DCs with either MIMLh5 or n-MIMLh5 in the presence of cytochalasin D, an inhibitor of actin-dependent cytoskeleton rearrangement (23). We found that the presence of cytochalasin D significantly decreased IL-12p70 production (by 27%) when DCs were stimulated with MIMLh5, whereas it did not significantly affect the IL-12p70 levels when DCs were stimulated with n-MIMLh5 (Fig. 4A). In addition, pretreatment with cytochalasin D increased IL-10 production induced by MIMLh5 and n-MIMLh5 (Fig. 4B), whereas TNF-α levels were not significantly affected (Fig. 4C).

Endocytosis of *L. helveticus* MIMLh5 is partly dependent on the presence of S-layer protein on the bacterial surface. To study the endocytosis of *L. helveticus* MIMLh5 in DCs, we prepared Alexa Fluor 647-labeled MIMLh5 and n-MIMLh5 cells. Labeling was not equally efficient for the two bacteria, and thus flow cytometry data are not directly comparable. When DCs were pretreated with cytochalasin D before the addition of the two bacterial preparations, we observed major reductions in the numbers of fluorescent DCs (i.e., DCs that had internalized fluorescently labeled bacteria); however, the difference in the numbers of DCs positive for endocytosed bacteria between cytochalasin D-treated and untreated DCs was greater for intact MIMLh5 than for n-MIMLh5, indicating more pronounced endocytosis of MIMLh5 (Fig. 5).

To directly demonstrate the role of the S-layer in endocytosis, we coated fluorescent beads of a size resembling bacterial cell dimensions (~800 nm) with the isolated MIMLh5 S-layer protein (Sl-beads). The quantity of beads employed to prepare Sl-beads to be used in comparative/chasing experiments was estimated on the basis of the bead average mass and the volume of individual beads. In these experiments, we decided to use the beads at the same multiplicity of infection (MOI) as used for bacterial cells (MOIs of 5 and 50), even though it was not possible to assume that the amounts of S-layer protein on beads and the bacterial surface were comparable. The presence of the S-layer protein with the fluorescent beads was demonstrated by SDS-PAGE (Fig. 6A, lanes 2 to 5), which showed bands at around 45 kDa. The slightly greater apparent size of proteins detached from Sl-beads (Fig. 6A, lanes 6 to 9) may be related to the extensive unfolding associated with noncovalent interactions of proteins with polystyrene nanoparticles (24, 25).

Sl-beads and plain beads (i.e., fluorescently labeled beads without any protein coating) were added to DCs, and the proportions of cells taking up beads were evaluated by flow cytometry (DCs positive for endocytosed beads) (Fig. 6B). When DCs were incubated with plain beads at a MOI of 50, about 28% of them endocytosed the beads, and addition of cytochalasin D only marginally reduced this number (from 28% to 22%) (Fig. 6B and C), indicating that the majority of the beads were stuck on the DC
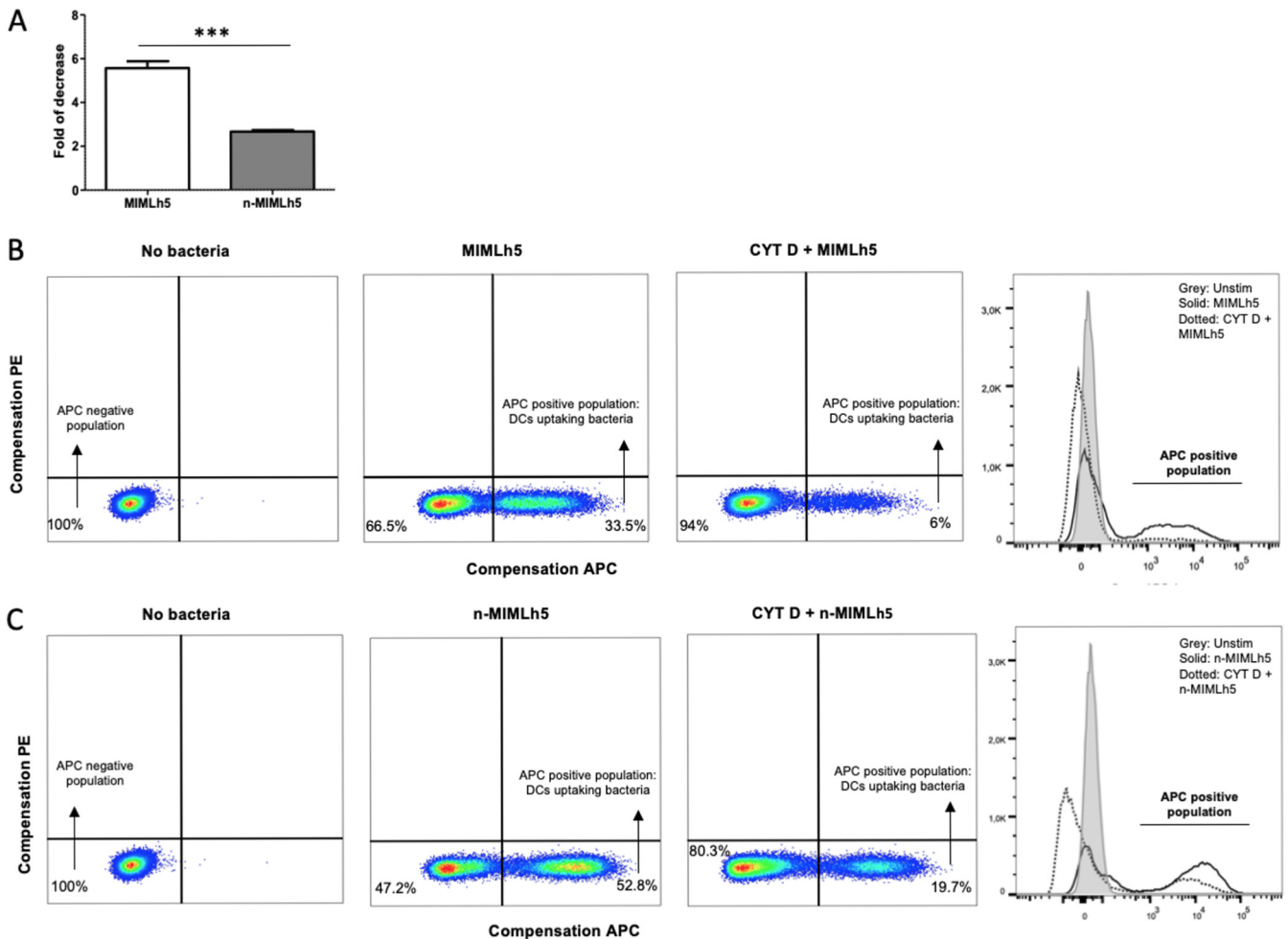
FIG 5 Flow cytometry analysis of DCs that had been pretreated with cytochalasin D or medium (no bacteria) for 1 h before stimulation with Alexa Fluor 647-labeled *L. helveticus* MIMLh5 for 30 min. (A) Data in the histograms are reported as fold decreases of the number of DCs positive for endocytosed MIMLh5 upon treatment with cytochalasin D, compared to untreated DCs. (B and C) Fluorescent untreated MIMLh5 cells (B) and n-MIMLh5 cells (C) were used at a MOI of 5. n-MIMLh5, MIMLh5 cells after removal of the S-layer protein by LiCl extraction. Allophycocyanin (APC)-positive population (emission spectrum of allophycocyanin and Alexa Fluor 647), DCs taking up bacteria. Asterisks indicate statistically significant differences, according to unpaired *t* tests. ***, $P < 0.001$. Dot plots are based on 50,000 cells counted on a FACS Cantoll system, with single-cell gating using FSC-A/FSC-H. Means and standard deviations are based on technical replicates.

surface. Conversely, incubation with Sl-beads at a MOI of 50 gave a higher percentage of positive DCs, compared to incubation with plain beads (53% positive), an effect that was also evident at a MOI of 5 (13% positive DCs in the presence of Sl-beads versus 5% in the presence of plain fluorescent beads) (Fig. 6B and D). The addition of cytochalasin D prior to the addition of Sl-beads reduced the proportion of positive DCs from 13% to 8% at a MOI of 5 and from 53% to 35% at a MOI of 50 (Fig. 6B to D), indicating decreased internalization of coated beads, compared to plain beads.

DISCUSSION

Here we demonstrated that depletion of the S-layer from *L. helveticus* MIMLh5 significantly reduced the capability of the bacteria to induce IFN-β, IL-12p70, and IL-10 expression in bone-marrow-derived DCs. In contrast, no major reduction in levels of the innate proinflammatory cytokines TNF-α and IL-1β was seen. The S-layer, as an isolated molecule, was a poor immune stimulator, inducing only weak expression of the cytokines IL-10, TNF-α, and IL-1β, and was unable to activate the expression of IFN-β and IL-12p70, even if we calculated that the amount of purified S-layer used was approximately 100 times greater than the S-layer present on the bacterial surfaces of
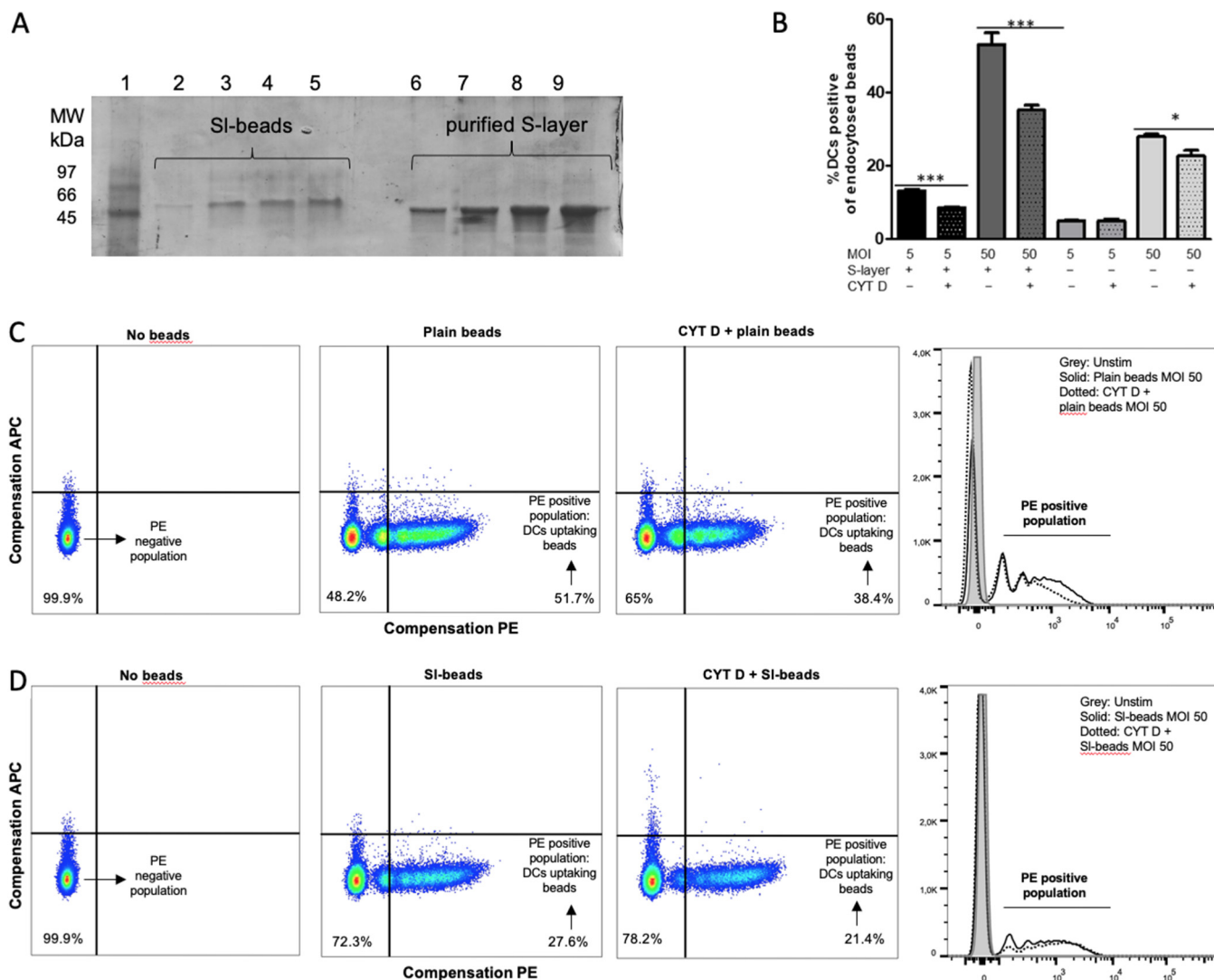
FIG 6 Effects of the presence of S-layer protein from MIMLh5 on polystyrene bead preparations, as revealed by SDS-PAGE with Coomassie blue staining, on endocytosis in DCs. (A) Lanes 2 to 5, Sl-beads at estimated MOIs of 20, 30, 40, and 50, respectively. Lanes 6 to 9, S-layer protein at 5, 10, 15, and 20 μg, respectively. DCs were pretreated with cytochalasin D or medium (no beads) for 1 h before stimulation with fluorescent beads for 1 h, followed by flow cytometry analysis. (B, C, and D) The percentage of DCs with endocytosed beads by macropinocytosis is indicated as a percentage of DCs positive for endocytosed beads (B). Fluorescent plain beads (B and C) and Sl-beads (B and D) were used at corresponding MOIs of 5 and 50. R-phycoerythrin (PE)-positive population (emission spectrum of R-phycoerythrin), DCs taking up beads. Asterisks indicate statistically significant differences, according to unpaired t tests. ***, $P < 0.001$; *, $P < 0.05$. Dot plots are based on 50,000 cells counted on a FACS Cantoll system, with single-cell gating using FSC-A/FSC-H. Means and standard deviations are based on technical replicates.

the amount of cells used in the same experiment. Because we demonstrated previously that induction of IFN-β by lactobacilli takes place in endosomes upon endocytosis of intact bacteria (16, 21), we hypothesized that the S-layer plays a key role in the endocytosis of the bacteria. We observed previously that lactobacilli can induce IL-12p70 by at least two distinct signaling pathways. One pathway depends on the induction of IFN-β through a MAPK pathway inducing c-Jun/ATF2 activation of AP-1, which is fully dependent on the MAPK JNK1/2 and, to much lesser degree, on p38; the MAPK ERK does not seem to be involved (17, 21). The other pathway leads to direct induction of IL-12p70 and seems to depend on p38 (21, 26).

Accordingly, we investigated how MAPK inhibitors of JNK1/2, p38, and ERK1/2 (via MEK) affected the IL-12p70 response upon stimulation with MIMLh5 or n-MIMLh5. The two bacterial stimulations demonstrated comparable effects regarding sensitivity to JNK1/2 inhibition. In contrast, inhibition of p38 resulted in a marked IL-12p70 decrease

after n-MIMLh5 stimulation, whereas the greatest sensitivity to IL-12p70 inhibition by ERK1/2 was observed after stimulation with native untreated MIMLh5. This finding led us to conclude that the S-layer depletion from MIMLh5 lowers its ability to promote IFN-β-mediated IL-12p70 production. We hypothesized that this might be due to impaired endocytosis of the S-layer-depleted bacteria. This idea is supported by experiments with cytochalasin D-treated DCs, which are unable to endocytose bacteria; the response induced by MIMLh5 was significantly reduced by cytochalasin D pretreatment, in contrast to n-MIMLh5. Similarly, we found greater β-actin-dependent uptake of fluorescently labeled MIMLh5 than of fluorescently labeled n-MIMLh5. Because we demonstrated previously that another S-layer-coated bacterium, *L. acidophilus* NCFM, is endocytosed partly by phagocytosis and partly by macropinocytosis in murine DCs (18), the difference between MIMLh5 and n-MIMLh5 in endocytosis by DCs in the presence of cytochalasin D may indicate that the S-layer-depleted bacteria are restricted in uptake by one of these mechanisms, most probably phagocytosis. A comparison of the cytochalasin D effects on endocytosis and IL-12p70 production indicates that only some of the IL-12p70 produced is dependent on endocytosis of the bacteria. Along the same lines, the decrease in IFN-β levels in DCs stimulated with S-layer-depleted MIMLh5 was not complete, which may indicate that some bacteria are still endocytosed by the constitutive micropinocytosis that takes place independently from the cell wall structures present on the bacterial cells. We showed previously that only a portion of endocytosed *L. acidophilus* NCFM is taken up by phagocytosis, while the rest was taken up by macropinocytosis (18, 27). The relevance of each event would depend on the properties of the bacteria and most notably on the bacterial surface, as well as on ceramide formation on the plasma membrane of DCs (18, 27, 28).

Because it was not possible to obtain a mutant lacking S-layer protein for *L. helveticus* MIMLh5, we used LiCl to efficiently remove the protein from the bacterial surface. However, this kind of treatment might also have affected other surface properties of *L. helveticus*, e.g., by removing other minor proteins and/or exposing other ligands. As already described, however, the S-layer is the most abundant protein on the bacterial cell surface, covering all of the bacterial wall, and its removal is plausibly the major outcome of LiCl treatment, as also evidenced by the disappearance of its band in SDS gels while the presence and intensity of other major proteins bands were left unaffected. Therefore, our hypothesis is about the role of the S-layer as the molecule recognized by phagocytosis-inducing receptors, and its removal could be the main reason for the reduced phagocytosis of *L. helveticus* by DCs and subsequent changes in endocytosed bacteria inducing cytokine production.

To support this hypothesis, we tried to coat fluorescent beads of a size comparable to bacteria with the isolated S-layer protein, in order to investigate whether this would facilitate endocytosis of the beads. We found a significantly greater number of bead-positive DCs when S-layer-coated beads were added, compared to the addition of plain fluorescent beads. This finding supports a role of the S-layer in facilitating endocytosis. The naked beads are readily dispersed in water solutions with medium ionic strength but at physiological pI, as used in this study, they may show some tendency to aggregate. Associations with S-layer proteins are likely to change this property toward more readily dispersed particles at physiological ionic strength. From this study, we cannot establish whether the greater uptake of S-layer-associated beads is due to binding to a specific receptor, stronger nonspecific attraction to the negatively charged cell surface, or greater dispensability. However, together with the results on the effects of S-layer-depleted MIMLh5, these data support a role of the S-layer in the endocytosis of MIMLh5. In summary, we have provided evidence that the S-layer of *L. helveticus* MIMLh5 is involved in the endocytosis of the bacterium, which is important for strong Th1-inducing cytokine production. Moreover, this kind of knowledge can be of help in the selection of probiotic strains for specific purposes, e.g., in cases of exacerbated IgE production, allergies, and atopy, where favoring a Th1 response would be of benefit.

MATERIALS AND METHODS

***L. helveticus* MIMLh5 preparation and growth conditions.** *L. helveticus* MIMLh5 was grown in de Man-Rogosa-Sharpe (MRS) broth (Difco Laboratories Inc., Detroit, MI, USA), inoculated from frozen glycerol stocks, and subcultured twice in MRS broth using 1:100 inocula. To prepare cultures to be used in immunological experiments, bacteria from an overnight culture were collected, washed twice with sterile phosphate-buffered saline (PBS), counted with a Neubauer counting chamber, resuspended at a concentration of 5×10^9 cells ml^{-1} in PBS, and stored in aliquots at $-80°$C. For preparation of n-MIMLh5, the cell pellet obtained after LiCl treatment (described below) was collected, washed three times with PBS to remove residual LiCl, resuspended in PBS, counted and brought to the same cell concentration as MIMLh5, and stored in aliquots at $-80°$C.

Extraction, purification, and chemical characterization of the S-layer protein from *L. helveticus* MIMLh5. Extraction of the S-layer protein from *L. helveticus* MIMLh5 was performed with high-molarity LiCl as described previously (7, 29). Briefly, cells from 500 ml of an overnight culture of MIMLh5 were harvested by centrifugation at $10,000 \times g$ for 20 min at 4°C and washed with 1 volume of cold sterile Milli-Q water. The cell pellet was extracted with 0.1 volume (referred to the starting broth culture volume) of 1 M LiCl for 30 min at room temperature in the presence of a protease inhibitor cocktail (Sigma-Aldrich, Darmstadt, Germany), with slight agitation. After centrifugation, the pellet was extracted with 0.1 volume of 5 M LiCl for 1 h at room temperature in the presence of protease inhibitor cocktail and centrifuged. The residual pellet was used to prepare n-MIMLh5 cells (described above), whereas the supernatant was filtered through a 0.2-μm filter and exhaustively dialyzed for 36 h at 4°C against distilled water containing 0.001% protease inhibitor cocktail. Dialysis was carried out with 12,000-kDa-cutoff membranes (Sigma-Aldrich) that had been previously boiled in 2% NaHCO$_3$, 1 mM EDTA. The dialysate was collected and centrifuged at $20,000 \times g$ for 20 min at 4°C. The supernatant was removed, and the pellet was resuspended in sterile Milli-Q water and freeze-dried. The lyophilized pellet was then resuspended at a concentration of 1 mg ml^{-1} in PBS and stored as aliquots at $-80°$C. Protein purity was determined by SDS-PAGE and reverse-phase high-performance liquid chromatography-electrospray ionization mass spectrometry analysis, as described previously (7). For SDS-PAGE, S-layer protein and total bacterial lysates were resuspended in SDS-PAGE (Laemmli) sample buffer, boiled for 5 min, and separated on 10% polyacrylamide gels in Tris-glycine-SDS buffer with a Mini-Protean 3 system (Bio-Rad). Gels were stained with Coomassie brilliant blue G-250 (Sigma-Aldrich, St. Louis, MO, USA).

Generation of bone-marrow-derived DCs. Bone-marrow-derived DCs were prepared as described previously (30). Briefly, bone marrow from C57BL/6 mice (Taconic, Lille Skensved, Denmark) was flushed out from the femur and tibia and washed. Bone marrow cells were seeded at 3×10^5 cells ml^{-1} in 10-cm petri dishes, in 10 ml RPMI 1640 medium (Sigma-Aldrich) containing 10% (vol/vol) heat-inactivated fetal calf serum (FCS) and supplemented with penicillin (100 U ml^{-1}), streptomycin (100 mg ml^{-1}), glutamine (4 mM), 50 mM 2-mercaptoethanol (all purchased from Cambrex BioWhittaker), and 15 ng ml^{-1} murine granulocyte-macrophage colony-stimulating factor (GM-CSF) (harvested from a GM-CSF-transfected Ag8.653 myeloma cell line). The cells were incubated for 8 days at 37°C in a humidified 5% CO$_2$ atmosphere. On day 3, 10 ml of complete medium containing 15 ng ml^{-1} GM-CSF was added. On day 6, 10 ml was removed and replaced with fresh medium. Nonadherent immature DCs were harvested on day 8.

Stimulation of DCs with bacterial cells, bacterial molecules, and beads. Immature DCs (2×10^6 cells ml^{-1}) were resuspended in fresh medium supplemented with 10 ng ml^{-1} GM-CSF, and 500 μl well^{-1} of DC suspension was seeded in 48-well tissue culture plates (Nunc, Roskilde, Denmark). *Lactobacillus helveticus* MIMLh5 was tested at MOIs of 5 and 50. S-layer protein from *L. helveticus* MIMLh5 was used at 10 μg ml^{-1}. Lipopolysaccharide (LPS) from *Escherichia coli* (Sigma-Aldrich) was used in all experiments as an internal control, at 1 μg ml^{-1} (data not shown). Uncoated beads and S-layer-coated beads were used at corresponding MOIs of 5 and 50 for ELISA experiments. Cytochalasin D (Sigma-Aldrich) was added at a concentration of 0.5 μg ml^{-1} 1 h prior to the incubation of DCs with bacteria. In the MAPK inhibition experiments, DCs (2×10^6 cells ml^{-1}) were preincubated for 1 h with (i) SP600125, a specific inhibitor of JNK1/2 (final concentration, 25 μM; InvivoGen, San Diego, CA, USA), (ii) SB203580, a specific inhibitor of p38 MAPK (final concentration, 10 μM; InvivoGen), or (iii) the MEK1/2 inhibitor U0126, which blocks MEK1/2 and thereby phosphorylation of the target ERK1/2 (final concentration, 10 μM; Cell Signaling Technology, Danvers, MA, USA). Under all of the conditions described, DCs and stimuli were incubated at 37°C in 5% CO$_2$. For time course experiments, DCs were harvested for RNA extraction after 2, 4, 6, and 10 h; the supernatants for ELISA analysis were collected after 4, 6, 10, and 20 h. In the other experiments, DCs were harvested for RNA extraction after 4 or 6 h and the supernatants for ELISA analysis after 20 h.

Cytokine quantification in DC supernatants. The concentrations of IL-12p70, IL-10, TNF-α, and IL-1β were analyzed by using commercially available ELISA antibody pairs (R&D Systems, Minneapolis, MN, USA) and the concentrations of IFN-β with an ELISA kit from PBL Assay Science (Piscataway, NJ, USA), according to the manufacturers' instructions.

RNA extraction. Murine bone-marrow-derived DCs were harvested and total RNA was extracted using the MagMAX sample separation system (Applied Biosystems, Foster City, CA, USA), including a DNase treatment step for genomic DNA removal. RNA concentrations were determined with a NanoDrop system (Thermo Fisher Scientific, Wilmington, DE, USA).

RT-qPCR. Five hundred nanograms of total RNA was reverse transcribed with the TaqMan reverse transcription reagent kit (Applied Biosystems, Foster City, CA, USA) using random hexamer primers, according to the manufacturer's instructions. The cDNA obtained was stored in aliquots at $-80°$C. Primers and probes were obtained and sequenced as described previously (18, 21, 31). qPCR amplifica-

tions were carried out in a total volume of 10 μl containing 1$\times$ TaqMan universal PCR master mix (Applied Biosystems), forward and reverse primers, TaqMan minor groove binder (MGB) probe, and the purified target cDNA (6 ng). Cycling was initiated for 20 s at 95°C, followed by 40 cycles of 3 s at 95°C and 30 s at 60°C, using an ABI Prism 7500 system (Applied Biosystems). Amplification reactions were performed in triplicate, and DNA contamination controls were included. The amplification results were normalized to the expression of the β-actin-encoding gene. Relative transcript levels were calculated by using the $2^{-\Delta\Delta CT}$ method (32).

Preparation of fluorescently labeled bacteria. For endocytosis experiments, untreated or S-layer-depleted *L. helveticus* MIMLh5 cells were fluorescently labeled using Alexa Fluor 647-conjugated succinimidyl esters (SE-AF647) (Molecular Probes, Eugene, OR, USA). Bacterial cells in Dulbecco's PBS (DPBS) were centrifuged for 5 min at 13,000 $\times$ *g* in 1.5-ml Eppendorf tubes and resuspended in 750 μl of sodium carbonate buffer (pH 8.5), and then SE-AF647 was added (10 μl for approximately 2 $\times$ 10^9 bacterial cells ml^{-1}). Bacteria were incubated at room temperature for 1 h in the dark with agitation, washed three times in sodium carbonate buffer, and finally resuspended in the original volume of DPBS.

Preparation of FITC-conjugated S-layer. The purified S-layer from *L. helveticus* MIMLh5 was dissolved in 5 M LiCl to obtain a 2-mg ml^{-1} protein solution, and the pH was adjusted to 9 by adding diluted NaOH. One milliliter of the protein solution was treated with 0.05 ml of a 1-mg ml^{-1} fluorescein isothiocyanate (FITC) solution in dimethyl sulfoxide. The reaction was carried out overnight at 4°C and stopped by adding 9 ml of 5 M urea in water. The FITC-conjugated protein solution was concentrated to 1 ml, while exchanging the buffer to 5 M urea, by using an Amicon Ultra-15 centrifugal filter unit (10-kDa cutoff; Merck Millipore Ltd., Cork, Ireland). The FITC-labeled protein was stored at 4°C.

S-layer adsorption on polystyrene nanoparticles. Fifty micrograms of Nile red fluorescent polystyrene nanoparticles, with an average size of 0.84 μm (Kisker Biotech, Steinfurt, Germany), were added to 1 ml of a 0.2-mg ml^{-1} FITC-labeled S-layer solution in 5 M urea and gently stirred at 4°C for 2 h. Then, the nanoparticle suspension was slowly diluted to a final volume of 10 ml by progressive addition of water over several hours. The preparation was kept overnight at 4°C, with stirring, and was centrifuged at 10,000 $\times$ *g* for 30 min at 4°C. The precipitated nanoparticles were washed three times with 5 M urea to remove unbound proteins, and the S-layer-coated nanoparticles were suspended in 1 ml of ultrapure water.

Evaluation of *L. helveticus* MIMLh5 and Sl-bead uptake by DCs. Nonadherent immature DCs were harvested and resuspended in complete medium to a concentration of 2 $\times$ 10^6 cells ml^{-1}. Pretreatment of cells with cytochalasin D (Sigma-Aldrich) at a final concentration of 0.5 μg ml^{-1} was performed in flasks at 37°C in a humidified 5% CO$_2$ atmosphere for 1 h before the addition of stimuli. Then 150 μl of DCs was seeded (3 $\times$ 10^5 cells well^{-1}) in 96-well, U-bottom, tissue culture plates (Nunc) and incubated with either fluorescent beads (uncoated or S-layer coated) or fluorescently labeled *L. helveticus* MIMLh5 (with or without a S-layer protein coating) for 30 min at 37°C in a humidified 5% CO$_2$ atmosphere. Bacteria were used at a MOI of 5, and beads were tested at MOIs of 5 and 50. All conditions were tested in triplicate, in at least three different experiments. Before each experiment, beads were treated in an ultrasound bath for at least 2 min, to gently ensure size uniformity. All of the stimuli were tested in the absence and presence of cytochalasin D. Controls included untreated cells and cells incubated only with cytochalasin D, without any stimulus. After incubation with beads and bacteria, DCs were centrifuged (1,200 $\times$ *g* for 5 min at 4°C), washed twice with cold PBS containing 1% FCS (washing buffer), and then fixed with 1% formaldehyde in washing buffer. Cells were analyzed by flow cytometry on a FacsCantoII system (BD Biosciences). Unless otherwise stated, data are from at least three independent experiments. Data analysis was performed using FlowJo 10 software (Ashland, OR, USA).

Statistical analysis. Statistical calculations were performed using the software program GraphPad Prism 5. The significance of the results was analyzed by unpaired heteroscedastic Student's *t* test with two-tailed distribution. Differences with *P* values of <0.05 were considered significant.

Ethics statement. All animals used as a source of bone marrow cells were housed under conditions approved by the Danish Animal Experiments Inspectorate (Forsøgdyrstilsynet), Ministry of Justice, Denmark, and experiments were carried out in accordance with the Council of Europe guidelines (33). Since the animals were used as sources of cells and no live animals were used in experiments, no specific approval was required for this study. Therefore, the animals used for this study are included in the general facility approval for the Faculty of Health and Medical Sciences, University of Copenhagen.

REFERENCES

1. Fagan RP, Fairweather NF. 2014. Biogenesis and functions of bacterial S-layers. Nat Rev Microbiol 12:211–222. https://doi.org/10.1038/nrmicro3213.
2. Zhu C, Guo G, Ma Q, Zhang F, Ma F, Liu J, Xiao D, Yang X, Sun M. 2017. Diversity in S-layers. Prog Biophys Mol Biol 123:1–15. https://doi.org/10.1016/j.pbiomolbio.2016.08.002.
3. Hynönen U, Palva A. 2013. *Lactobacillus* surface layer proteins: structure, function and applications. Appl Microbiol Biotechnol 97:5225–5243. https://doi.org/10.1007/s00253-013-4962-2.
4. Sun Z, Kong J, Hu S, Kong W, Lu W, Liu W. 2013. Characterization of a S-layer protein from *Lactobacillus crispatus* K313 and the domains responsible for binding to cell wall and adherence to collagen. Appl Microbiol Biotechnol 97:1941–1952. https://doi.org/10.1007/s00253-012-4044-x.

5. de Leeuw E, Li X, Lu W. 2006. Binding characteristics of the *Lactobacillus brevis* ATCC 8287 surface layer to extracellular matrix proteins. FEMS Microbiol Lett 260:210–215. https://doi.org/10.1111/j.1574-6968.2006.00313.x.

6. Lightfoot YL, Selle K, Yang T, Goh YJ, Sahay B, Zadeh M, Owen JL, Colliou N, Li E, Johannssen T, Lepenies B, Klaenhammer TR, Mohamadzadeh M. 2015. SIGNR3-dependent immune regulation by *Lactobacillus acidophilus* surface layer protein A in colitis. EMBO J 34:881–895. https://doi.org/10.15252/embj.201490296.

7. Taverniti V, Stuknyte M, Minuzzo M, Arioli S, De Noni I, Scabiosi C, Cordova ZM, Junttila I, Hämäläinen S, Turpeinen H, Mora D, Karp M, Pesu M, Guglielmetti S. 2013. S-layer protein mediates the stimulatory effect of *Lactobacillus helveticus* MIMLh5 on innate immunity. Appl Environ Microbiol 79:1221–1231. https://doi.org/10.1128/AEM.03056-12.

8. Li P, Yu Q, Ye X, Wang Z, Yang Q. 2011. *Lactobacillus* S-layer protein inhibition of *Salmonella*-induced reorganization of the cytoskeleton and activation of MAPK signalling pathways in Caco-2 cells. Microbiology 157:2639–2646. https://doi.org/10.1099/mic.0.049148-0.

9. Konstantinov SR, Smidt H, de Vos WM, Bruijns SC, Singh SK, Valence F, Molle D, Lortal S, Altermann E, Klaenhammer TR, van Kooyk Y. 2008. S layer protein A of *Lactobacillus acidophilus* NCFM regulates immature dendritic cell and T cell functions. Proc Natl Acad Sci U S A 105:19474–19479. https://doi.org/10.1073/pnas.0810305105.

10. Taverniti V, Dalla Via A, Minuzzo M, Del Bo' C, Riso P, Frøkiær H, Guglielmetti S. 2017. In vitro assessment of the ability of probiotics, blueberry and food carbohydrates to prevent *S. pyogenes* adhesion on pharyngeal epithelium and modulate immune responses. Food Funct 8:3601–3609. https://doi.org/10.1039/c7fo00829e.

11. Taverniti V, Minuzzo M, Arioli S, Junttila I, Hämäläinen S, Turpeinen H, Mora D, Karp M, Pesu M, Guglielmetti S. 2012. In vitro functional and immunomodulatory properties of the *Lactobacillus helveticus* MIMLh5-*Streptococcus salivarius* ST3 association that are relevant to the development of a pharyngeal probiotic product. Appl Environ Microbiol 78:4209–4216. https://doi.org/10.1128/AEM.00325-12.

12. Guglielmetti S, Taverniti V, Minuzzo M, Arioli S, Stuknyte M, Karp M, Mora D. 2010. Oral bacteria as potential probiotics for the pharyngeal mucosa. Appl Environ Microbiol 76:3948–3958. https://doi.org/10.1128/AEM.00109-10.

13. Guglielmetti S, Taverniti V, Minuzzo M, Arioli S, Zanoni I, Stuknyte M, Granucci F, Karp M, Mora D. 2010. A dairy bacterium displays in vitro probiotic properties for the pharyngeal mucosa by antagonizing group A streptococci and modulating the immune response. Infect Immun 78:4734–4743. https://doi.org/10.1128/IAI.00559-10.

14. Savina A, Amigorena S. 2007. Phagocytosis and antigen presentation in dendritic cells. Immunol Rev 219:143–156. https://doi.org/10.1111/j.1600-065X.2007.00552.x.

15. Liu Z, Roche PA. 2015. Macropinocytosis in phagocytes: regulation of MHC class-II-restricted antigen presentation in dendritic cells. Front Physiol 6:1–6. https://doi.org/10.3389/fphys.2015.00001.

16. Weiss G, Rasmussen S, Zeuthen LH, Nielsen BN, Jarmer H, Jespersen L, Frøkiaer H. 2010. *Lactobacillus acidophilus* induces virus immune defence genes in murine dendritic cells by a Toll-like receptor-2-dependent mechanism. Immunology 131:268–281. https://doi.org/10.1111/j.1365-2567.2010.03301.x.

17. Weiss G, Rasmussen S, Nielsen Fink L, Jarmer H, Nøhr Nielsen B, Frøkiær H. 2010. *Bifidobacterium bifidum* actively changes the gene expression profile induced by *Lactobacillus acidophilus* in murine dendritic cells. PLoS One 5:e11065. https://doi.org/10.1371/journal.pone.0011065.

18. Boye L, Welsby I, Lund LD, Goriely S, Frøkiaer H. 2016. Plasma membrane Toll-like receptor activation increases bacterial uptake but abrogates endosomal *Lactobacillus acidophilus* induction of interferon-β. Immunology 149:329–342. https://doi.org/10.1111/imm.12650.

19. Stuknyte M, Brockmann EC, Huovinen T, Guglielmetti S, Mora D, Taverniti V, Arioli S, De Noni I, Lamminmäki U. 2014. *Lactobacillus helveticus* MIMLh5-specific antibodies for detection of S-layer protein in Grana Padano protected-designation-of-origin cheese. Appl Environ Microbiol 80:694–703. https://doi.org/10.1128/AEM.03057-13.

20. Kaji R, Kiyoshima-Shibata J, Nagaoka M, Nanno M, Shida K. 2010. Bacterial teichoic acids reverse predominant IL-12 production induced by certain *Lactobacillus* strains into predominant IL-10 production via TLR2-dependent ERK activation in macrophages. J Immunol 184:3505–3513. https://doi.org/10.4049/jimmunol.0901569.

21. Weiss G, Christensen HR, Zeuthen LH, Vogensen FK, Jakobsen M, Frøkiær H. 2011. Lactobacilli and bifidobacteria induce differential interferon-β profiles in dendritic cells. Cytokine 56:520–530. https://doi.org/10.1016/j.cyto.2011.07.024.

22. Weiss G, Maaetoft-Udsen K, Stifter SA, Hertzog P, Goriely S, Thomsen AR, Paludan SR, Frøkiær H. 2012. MyD88 drives the IFN-β response to *Lactobacillus acidophilus* in dendritic cells through a mechanism involving IRF1, IRF3, and IRF7. J Immunol 189:2860–2868. https://doi.org/10.4049/jimmunol.1103491.

23. Cooper JA. 1987. Effects of cytochalasin and phalloidin on actin. J Cell Biol 105:1473–1478. https://doi.org/10.1083/jcb.105.4.1473.

24. Barbiroli A, Bonomi F, Iametti S, Marengo M. 2015. Stabilization of the "open" conformer of apoIscU on the surface of polystyrene nanobeads accelerates assembly of a 2Fe2S structure. Peptidomics 2:40–44. https://doi.org/10.1515/ped-2015-0006.

25. Miriani M, Iametti S, Kurtz DM, Bonomi F. 2014. Rubredoxin refolding on nanostructured hydrophobic surfaces: evidence for a new type of biomimetic chaperones. Proteins 82:3154–3162. https://doi.org/10.1002/prot.24675.

26. Lu HT, Yang DD, Wysk M, Gatti E, Mellman I, Davis RJ, Flavell RA. 1999. Defective IL12 production in mitogen-activated protein (MAP) kinase kinase 3 (Mkk3)-deficient mice. EMBO J 18:1845–1857. https://doi.org/10.1093/emboj/18.7.1845.

27. Fuglsang E, Boye L, Frøkiær H. 2017. Enhancement of ceramide formation increases endocytosis of *Lactobacillus acidophilus* and leads to increased IFN-β and IL-12 production in dendritic cells. J Clin Immunol Res 1:1–9.

28. Abdel Shakor AB, Kwiatkowska K, Sobota A. 2004. Cell surface ceramide generation precedes and controls FcγRII clustering and phosphorylation in rafts. J Biol Chem 279:36778–36787. https://doi.org/10.1074/jbc.M402170200.

29. Smit E, Oling F, Demel R, Martinez B, Pouwels PH. 2001. The S-layer protein of *Lactobacillus acidophilus* ATCC 4356: identification and characterisation of domains responsible for S-protein assembly and cell wall binding. J Mol Biol 305:245–257. https://doi.org/10.1006/jmbi.2000.4258.

30. Christensen HR, Frokiaer H, Pestka JJ. 2002. Lactobacilli differentially modulate expression of cytokines and maturation surface markers in murine dendritic cells. J Immunol 168:171–178. https://doi.org/10.4049/jimmunol.168.1.171.

31. Weiss G, Forster S, Irving A, Tate M, Ferrero RL, Hertzog P, Frøkiær H, Kaparakis-Liaskos M. 2013. *Helicobacter pylori* VacA suppresses *Lactobacillus acidophilus*-induced interferon beta signaling in macrophages via alterations in the endocytic pathway. mBio 4:e00609-12. https://doi.org/10.1128/mBio.00609-12.

32. Livak KJ, Schmittgen TD. 2001. Analysis of relative gene expression data using real-time quantitative PCR and the $2^{-\Delta\Delta CT}$ method. Methods 25:402–408. https://doi.org/10.1006/meth.2001.1262.

33. Council of Europe. 1986. European treaty series 123: European convention for the protection of vertebrate animals used for experimental and other scientific purposes. Council of Europe, Strasbourg, France.